



HAL
open science

Ab initio investigation of the relative stability of silicogermanates and their (Alumino)Silicates counterparts

Elsy El Hayek, Bogdan Harbuzaru, Johan A Martens, Céline Chizallet

► **To cite this version:**

Elsy El Hayek, Bogdan Harbuzaru, Johan A Martens, Céline Chizallet. Ab initio investigation of the relative stability of silicogermanates and their (Alumino)Silicates counterparts. *Microporous and Mesoporous Materials*, 2020, 306, pp.110425. 10.1016/j.micromeso.2020.110425 . hal-02953954

HAL Id: hal-02953954

<https://ifp.hal.science/hal-02953954>

Submitted on 30 Sep 2020

HAL is a multi-disciplinary open access archive for the deposit and dissemination of scientific research documents, whether they are published or not. The documents may come from teaching and research institutions in France or abroad, or from public or private research centers.

L'archive ouverte pluridisciplinaire **HAL**, est destinée au dépôt et à la diffusion de documents scientifiques de niveau recherche, publiés ou non, émanant des établissements d'enseignement et de recherche français ou étrangers, des laboratoires publics ou privés.

Ab Initio Investigation of the Relative Stability of Silicogermanates and Their (Alumino)Silicates Counterparts

Elsy El Hayek,^{a,b} Bogdan Harbuzaru,^a Johan A. Martens,^b Céline Chizallet^{a*}

^a IFP Energies nouvelles-Etablissement de Lyon, Rond-point de l'échangeur de Solaize, 69360, Solaize, France.

^b Center for Surface Chemistry and Catalysis, KU Leuven, Celestijnenlaan 200F, 3001 Leuven, Belgium.

Corresponding Author :

* Céline Chizallet, IFP Energies nouvelles, celine.chizallet@ifpen.fr

Abstract:

The diversity of synthetic zeolites with silicogermanate composition has grown significantly. Many of these zeolites have large pores, thanks to the double 4-ring (d4r) structural subunits occupied by Ge atoms. The wide pores make them potentially interesting for catalytic transformation of bulky molecules, but the thermal and hydrothermal stability and the acidity are insufficient for practical applications. In the present work, the stability of known silicogermanate zeolite structures and their silicate and aluminosilicate analogues is evaluated using periodic density functional theory calculations. The thermodynamics of isomorphic substitution of Ge atoms for Si and Al via chemical processes are investigated. The study reveals that thermodynamically, (alumino)silicate counterparts of all known silicogermanates are intrinsically stable, and that the energetics of isomorphic substitution reactions of Ge atoms are almost independent of the distribution of d4r units in the different framework topologies. Chlorides are found better isomorphic substitution reagent candidates, at least theoretically. This work opens perspectives for the catalytic use of stable derivatives of silicogermanate zeolites.

Keywords: Zeolite, silicogermanate, post-treatment, stabilization, DFT.

1. Introduction

The most useful synthetic zeolites for practical applications have aluminosilicate composition. Their microporous frameworks composed of three-dimensional arrangements of SiO_4 and AlO_4 tetrahedra can support strong acid sites and are thermally and hydrothermally stable enough for industrial processes in the fields of adsorption, catalysis, separation or ion exchange [1,2]. Incorporation of germanium in the zeolite framework favors the formation of smaller polyhedra such as double 4-rings d4r of tetrahedra [3–9]. This leads to the creation of new framework topologies, sometimes with wide pores of interest to adsorption and catalysis. It explains the interest in these materials from both academic and industrial perspectives.

Silicogermanate zeolites are synthesized using organic template molecules. As soon as these templates are removed through calcination, the zeolite becomes unstable because exposure to ambient air humidity already causes hydrolysis of Ge-O bonds [4,7,10–12]. A scientific challenge is to find ways to substituting germanium for aluminum or silicon to generate stable structures. In order to stabilize these silicogermanates, two experimental post-treatment approaches have been developed in literature. The first approach allows the initial structure of the parent germanosilicate zeolite to be maintained. To this aim, Ge atoms need to be substituted directly by Al atoms [10,11,13,14]. This can be achieved through leaching of the zeolite with acid to dislodge the Ge atoms from the framework in the presence of an external Si or Al source [4,15–18]. In the second approach, the original framework is decomposed by breaking framework oxide bonds of Ge atoms. When the Ge atoms occupy specific crystallographic positions, this rupture of the network generates

structural subunits which are then rearranged and reconnected to new zeolite structures. This approach is used in ADOR (Assembly–Disassembly–Organisation–Reassembly) [19] and in the inverse sigma transformation [8,20].

Density functional theory (DFT) calculations have been used to study the stability of the ITQ-44 silicogermanate when Ge was substituted by different elements such as silicon, aluminum or zinc [21]. ITQ-44 zeolite framework was found to be stable in the absence of germanium, although to date a synthesis method for this zeolite type without Ge has not yet been reported. Computation has shown that theoretically incorporating aluminum into the ITQ-44 silicate zeolite is favorable. It predicts that it should be possible to obtain this zeolite in a silicate or aluminosilicate form either by direct synthesis or by post-synthesis treatment.

In the present work, we investigated the stability of all reported silicogermanate zeolite framework types as a basis of selection of candidates for future experimental studies on isomorphic substitution of Ge atoms by Al and Si. To this aim we investigated the intrinsic stability of silicogermanate zeolite types having structural codes attributed by the international zeolite association. Some silicogermanates already exist in aluminosilicate or silicate forms reflecting the stability of these structures such as AST [22–25], BEC [26–28], ISV [29–32], LTA [33–35], MFI [25,36,37] and STI [38,39], therefore we selected one of these structures, the BEC, while the rest have been excluded from the present study. The BEC zeolite was synthesized as a germanate [40], as an overgrown silicate crystal [27], as a pure silicate [26], as a silicogermanate [28] and the post-treatment of the pure BEC silicogermanate allowed successfully the partial substitution of Ge by Al [10]. Moreover,

the -CLO and -SYT structures are constructed exclusively by connected d4r units, while BEA, DFT, EWO, MFI and STI structures do not contain d4r units, as a consequence the strategy followed in this work (described in section 3.1) is not applicable and the seven structures were excluded. Thus 20 regular structures, [3,6,25,28,41–67,67–79] 4 interrupted [6,80–85] and 2 partially disordered [86–89] structures were studied. Note that the term ‘regular’ is used for fully ordered type materials, ‘interrupted’ is related to fully ordered type materials with systematic interruption in the framework such that not all T atoms are 4-connected to other T atoms. ‘Partially disordered’ refers to materials with disorders in terms of specific building units. Our calculations were performed in the framework of the periodic DFT with a dispersion-corrected exchange-correlation functional, to simulate the different structures with different compositions.

First we investigated whether the topologies are stable in silicate or aluminosilicate composition. Then we inspected the possibility of substituting Ge for another structural element such as Si or Al to verify which candidates can be stabilized by post-treatment.

2. Computational methods

2.1. Structures optimization

Periodic DFT calculations were performed using the Vienna ab initio simulation package (VASP) code [90,91] with the Perdew, Burke and Ernzerhof [92] (PBE, GGA family) exchange-correlation functional and a density dependent dispersion correction (dDsC) for the dispersion interactions [93]. The projected augmented wave (PAW) method [94] was used to describe the core electron interactions with a cut-off energy of 800 eV and of 400

eV for the geometry optimization of zeolites structures, with or without relaxation of the cell parameters respectively.

All initial zeolites structures were taken from the International Zeolite Association website [95]. Unit cell parameters were relaxed according to the following procedure:

- Step 1: Cell parameters are fixed while atoms are free (cutoff: 400 eV)
- Step 2: Atoms and cell parameters are free (cutoff: 800 eV)
- Step 3: Cell parameters are fixed while atoms are free (cutoff: 400 eV)

Geometry optimizations were continued until forces were lower than 0.02 eV/Å for steps 1 and 3 and until the energy difference between two consecutive optimization steps was lower than 10^{-4} eV for step 2. The break condition for the electronic SCF loop was fixed to 10^{-5} eV for all calculations. Gaussian smearing was set with a width of 0.05 eV. Table 1 reports all the investigated structures with the K-points mesh used for energy calculations. This approach was also applied on materials used as references: 2x2x2 supercells were used for an accurate estimation of the energy of silica quartz (K-points mesh: 3x3x3), germanium oxide rutile (3x3x4) and α -alumina (3x3x1). The electronic energies of water used as reference for interrupted structures was evaluated by placing a water molecule in a 25x25x25Å cell.

2.2. Calculations of substitution energies and free energies

Substitution energies and free energies of Ge atoms for Si or Al were quantified with respect to several sets of references: molecular hydroxides e.g. Si(OH)₄, Ge(OH)₄ and

Al(OH)₃(H₂O) or chlorides such as SiCl₄, GeCl₄ and AlCl₃. The energies of these molecules were evaluated by placing each molecule (1x1x1) in a 25x25x25 Å³ cell.

The energies of substitution when varying the amount and distribution of Ge were calculated from the energies of reactions presented in paragraph 3.2 below.

Substitution reactions occur at finite temperatures. Thus to obtain a more realistic description of experimental substitutions, statistical thermodynamics of these substitution reactions have been used to estimate the Gibbs free energy, $\Delta G_{\text{sub,Ge} \rightarrow \text{Si/Al}}$ (kJ/mol) by considering the rotational, translational, and vibrational degrees of freedom of isolated gas-phase molecules[96]. Vibrational properties of these molecules were determined by finite difference, with a displacement of ± 0.005 Å of each atom starting from the equilibrium position. The thermal contributions for condensed phases (silicates, aluminosilicates, silicogermanates) were neglected.

3. Results and discussion

3.1. Intrinsic stability of silicogermanates and their (alumino)silicates counterparts

The Ge distribution in silicogermanate zeolite frameworks is not well defined. It is known that high $\widehat{\text{SiOSi}}$ angle values lead to more stable solids than their corresponding $\widehat{\text{GeOSi}}$ and $\widehat{\text{GeOGe}}$ [97,98]. However, when it comes to narrower angles such as in d4rs, germanium assures the stabilization of these units by reducing their strain. Only after reaching a certain amount of Ge, the Ge starts to be located in sites corresponding to sufficient low angles, outside of the d4r [98]. Thus we limited our study to Ge occupying d4r units only. Based on experimental observations in literature, Ge atoms occupy mostly all T sites of the d4r, or

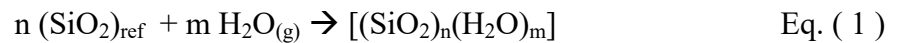
half of these [64]. Thus to model silicogermanates structures, we have considered three possibilities: Ge occupying all the T sites of the d4r (Figure 1a), Ge occupying half of the T sites of the d4r respecting alternation with Si (Figure 1b) and Ge occupying half of the T sites of the d4r in the same s4r (Figure 1c).

For aluminosilicates, respecting the Löwenstein rule [99] imposes that Al alternates with Si in the d4r. To compensate the negative charge induced by Al, one hydrogen atom is added for each Al (Figure 2).

The lattice parameters after geometry optimization of the different structures are reported in Table S1.

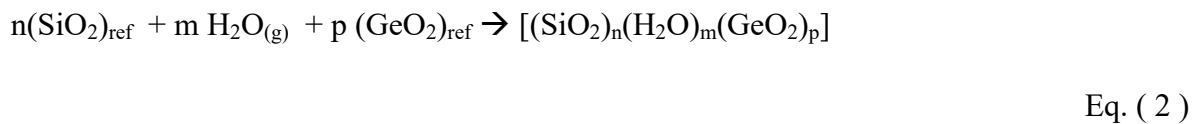
The intrinsic stabilities of the structures were evaluated through their energies of formation. Silica quartz, germanium oxide rutile and α -alumina were chosen as reference structures in our calculations. The energies of formation (ΔE_{form}) per T sites were calculated from the reaction energy of the following reactions:

❖ Silicates:



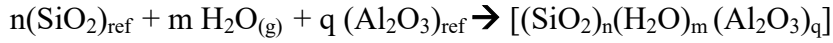
with $T = n$ (T being the total number of T sites),

❖ Silicogermanates with Ge occupying all the corners of d4r:



with $T = n+p$,

❖ Aluminosilicates:



Eq. (3)

with $T = n + 2q$.

Note that water is necessary ($m \neq 0$) only in the chemical reactions involving the formation of interrupted structures.

ΔE_{form} (kJ/mol) per T site for different structures is presented in Figure 3 and Table S1. These energies are all positive (with the exception of interrupted structures, see below), confirming that quartz, corundum and rutile are more stable polymorphs, as expected, whereas zeolites are metastable. Interestingly, it was shown that all silicates and aluminosilicates frameworks are more stable than the corresponding silicogermanates.

This result is in accordance with the experimental measurements of the enthalpies of formation per T sites of BEC materials free of connectivity defects where an increase from 17.79 ± 0.72 kJ/mol for the pure silica form [56] to 19.74 ± 0.32 and 21.04 ± 0.24 for silicogermanates with Si/Ge ratio of 3.5 and 1.4 respectively was detected [9]. The experimental enthalpies were calculated based on a high temperature oxide melt solution calorimetry from 298 to 973K using silica and germania quartz as references. In our calculations, the (electronic) energies of formation per T sites of BEC increase from 14 kJ/mol for pure silica, to 27 and to 37 kJ/mol for silicogermanate forms with Si/Ge of 3 and 1 respectively, considering the transformation in solid forms departing from silica quartz and germanium oxide rutile as reference structures at 0 K (Eq.1, 2 and 3). Note that the germanium oxide rutile was chosen over the α -quartz because of its higher stability [101], by 30 kJ/mol. Using α -quartz Germania as a reference, similar to experiments, the energies

of formation of BEC per T sites increase from 14 kJ/mol for pure silica, to 20 and to 22 kJ/mol for silicogermanate forms with Si/Ge of 3 and 1 respectively. This is in excellent agreement with experimental results. Moreover, previous measurements of the enthalpies of formation of ITQ-21 and ITQ-22 after varying the Ge amount, confirmed that silicogermanates forms are less stable than silicate zeolites [100]. This indicates that Ge is destabilizing the structure. The role of this element in the formation of large pore structures is thus of kinetic nature, providing more stable crystal growth intermediates in solution during the synthesis and in orienting the crystallization process to a specific structure. For example, increasing the Ge content favors the formation of ITQ-22 over the EU-1 zeolite [63].

The energies of formation of normal and disordered structures are correlated with the d4r content of the structure (Figure 3a). This result is congruent with earlier work by Wu et al [56] showing that the enthalpy of formation increased with increasing number of d4r in a series of zeolites, viz. ITQ-7, -17, -21, -22, and -33.

Interrupted aluminosilicates do not follow the general trend and have higher intrinsic stabilities compared to normal and disordered structures, with negative formation energies (Figure 3b). This may result from interactions between hydroxyls of interrupted frameworks and compensation hydrogen atoms, see Figure S1a. It can also be due to the reference state of water (gas phase) chosen for the calculation of the formation energy. Furthermore, the particular stability of the -ITV structure ($\Delta E_{\text{form}}/\text{T sites} = -89 \text{ kJ/mol}$) can be related to the location of all the interrupted sites on the d4r units (Figure S1b) while the -IFU, -IFT and -IRY structures have their interrupted sites on other rings (Figure S1a).

A trend between the framework density and the stability of zeolites was established by force field calculations performed on a large array of solids [102], indicating that zeolites with higher densities tend to be more stable. However, other force field and quantum calculations, [103,104] dealing with a lower number of structures, and experimental measurements [105] suggested a quasi-invariance of the stability with respect to the density, and that the only factor affecting the stability is the presence of 3-membered rings due to its strain. Above this size, the rings seem to be unstrained and to have similar stability.

Our results (Figure S2) support the independence of the intrinsic stability of silicogermanates and their densities. This independence is still valid for their aluminosilicate analogues. For silicates, the correlation is of better quality with respect to silicogermanates and aluminosilicates. As a consequence, we suggest that the intrinsic stability of all silicogermanates is rather independent of the framework density but is directly related to the Ge content. The latter element orients the crystallization process to new structures [106]. For instance, the competition between the growth of BEC, ISV and BEA type zeolites can be explained by relative stability changes depending on the Si/Ge ratio [107].

Another interesting aspect is the influence of the content and distribution of d4r units in the framework on its density. Figure 4 points out that the density is not directly related to the content of d4r. Even structures with the same number of d4r have different densities. This is quite pronounced for structures with $N_{d4r}/N_T = 0.1$ (Figure 4). In some cases, increasing the

number of d4r in the framework reduces the density of the structure, for example the IM-12 silicogermanate having a UTL framework has a framework density of 14.9 (T/1000Å³) and two d4r per unit cell, while the ITT structure with 3 d4r per unit cell has a lower framework density of 11.7 (T/1000Å³). The high framework density of UOZ of 17.45 (T/1000Å³) is in line with its high d4r content in the framework (4 d4r units per unit cell). Figure 5 sketches how the distribution of d4r in the structure affects the density: in UTL, the d4r are separating the layers and creating a spacious framework with reduced density while the UOZ structure, composed mainly of interconnected d4r, has a higher framework density. In consequence, one can say that density is affected by the arrangement of the d4rs and not by their amount in the framework. This reconfirms that the stability of silicogermanates is not directly related to the framework density.

Based on these results, silicate and aluminosilicate counterparts of silicogermanate zeolites are stable. However, most of these zeolites cannot be obtained by direct synthesis. They may be obtained by post-treatments. To estimate the possibility of these transformations, we have calculated the energies of substitution of Ge for Si and Al, considering various substitution agents.

3.2. Isomorphous substitution of Ge atoms for Si and Al

To investigate the possibility of substitution of Ge for Si and Al, hydroxide and chloride reactant molecules were used in the calculations. In the case of chlorides, the studied substitutions are represented in

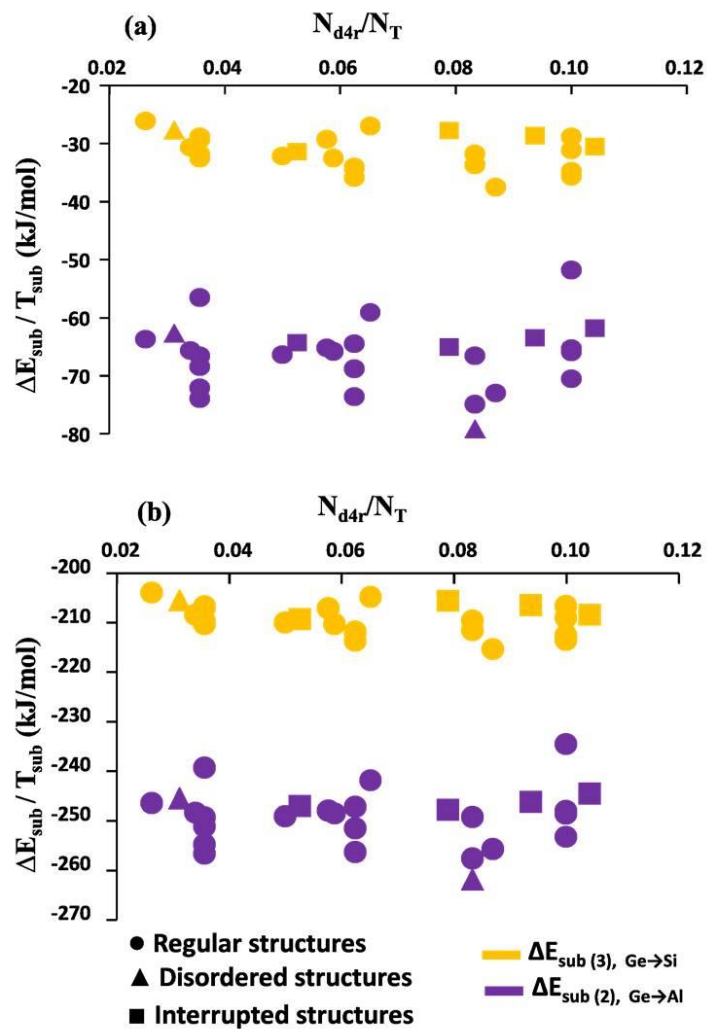


Figure 7: Energies of full substitution of Ge for Si ($\Delta E_{\text{sub}(3), \text{Ge} \rightarrow \text{Si}}$) departing from Ge occupying the full d4r (yellow) and of Ge for Al ($\Delta E_{\text{sub}(2), \text{Ge} \rightarrow \text{Al}}$) departing from Ge occupying half of the d4r with alternation (purple), normalized to the number of substituted T sites, using (a) hydroxides and (b) chlorides against the number of d4r in the structures over the total T sites (N_{d4r}/N_T). Spheres, triangles and squares correspond to regular, partially disordered and interrupted zeolite structures, respectively.

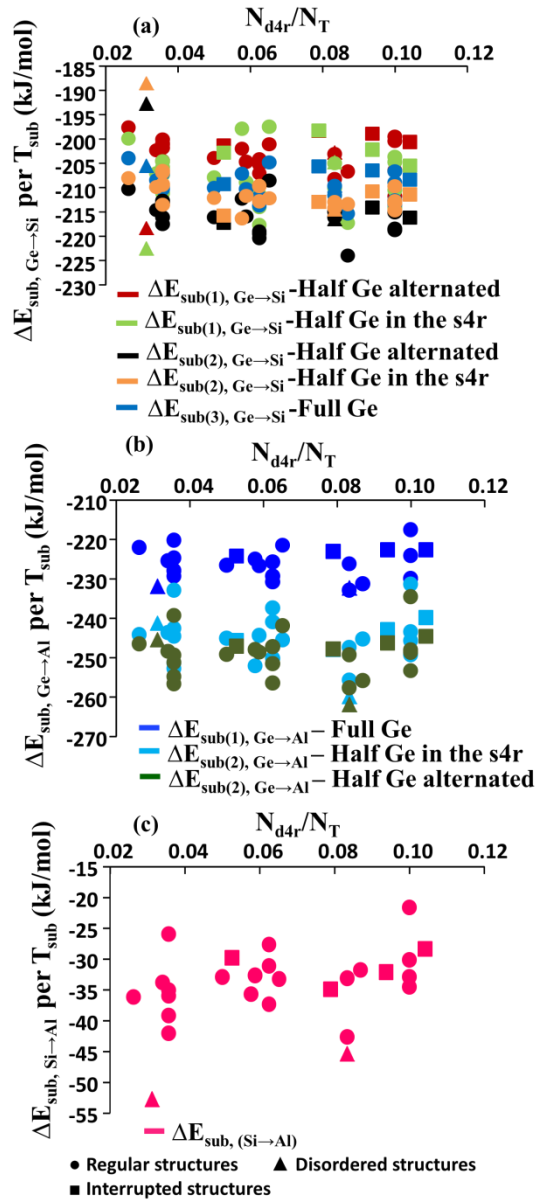


Figure 8: Energies of partial substitution of Ge for Si $\Delta E_{\text{sub}(1), \text{Ge} \rightarrow \text{Si}}$ departing from full occupation of d4r with Ge and full substitution $\Delta E_{\text{sub}(2,3), \text{Ge} \rightarrow \text{Si}}$ departing from Ge occupying half/same s4r and fully in the d4r respectively(a). Energies of partial substitution of Ge for Al $\Delta E_{\text{sub}(1), \text{Ge} \rightarrow \text{Al}}$ departing from Ge occupying the full d4r and full substitution $\Delta E_{\text{sub}(2), \text{Ge} \rightarrow \text{Al}}$ departing from Ge occupying half of the d4r with alternation or in the same s4r (b). Energies of full substitution of Si for Al $\Delta E_{\text{sub, Si} \rightarrow \text{Al}}$ departing from Al occupying half of the d4r (c). All the energies are normalized to the number of substituted T sites against the number of d4r in the structures over the total T sites (N_{d4r}/N_T). Spheres, triangles and squares correspond to regular, partially disordered and interrupted structures respectively.

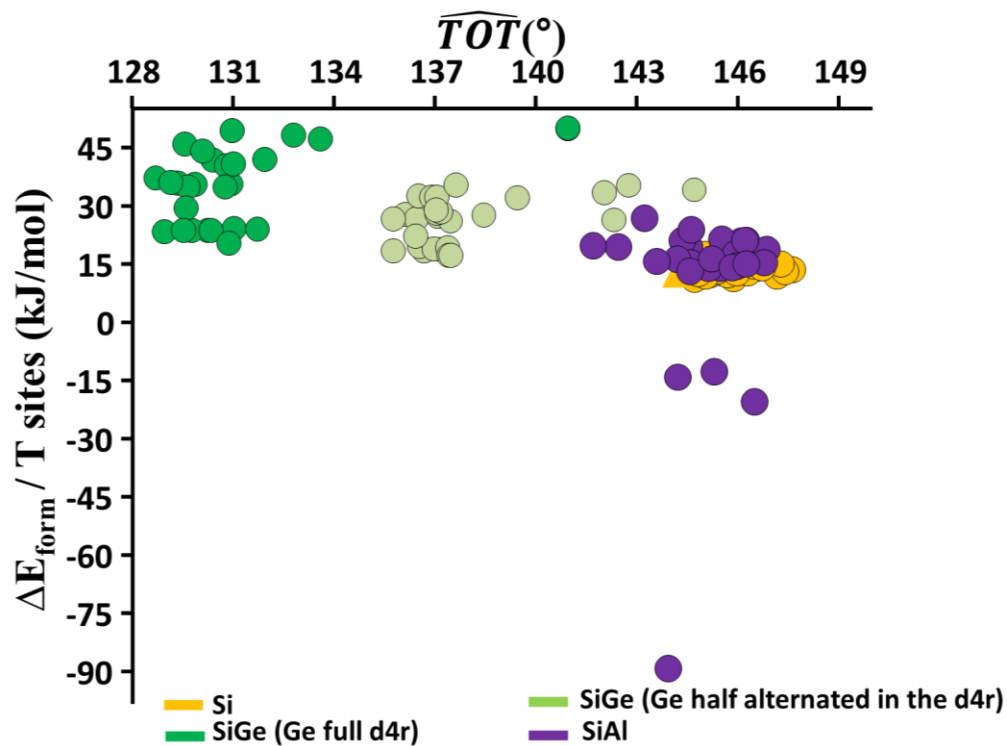


Figure 9: Energies of formation per T sites ($\Delta E_{\text{form}} / \text{T sites}$) of silicates (yellow), silicogermanates with Ge occupying the full d4r (dark green)/ Ge occupying half of the d4r with alternation (light green) and aluminosilicates (purple) of all studied structures. \widehat{TOT} correspond to angles in the d4r respectively \widehat{SiOSi} , \widehat{GeOGe} , \widehat{SiOGe} and \widehat{SiOAl} .

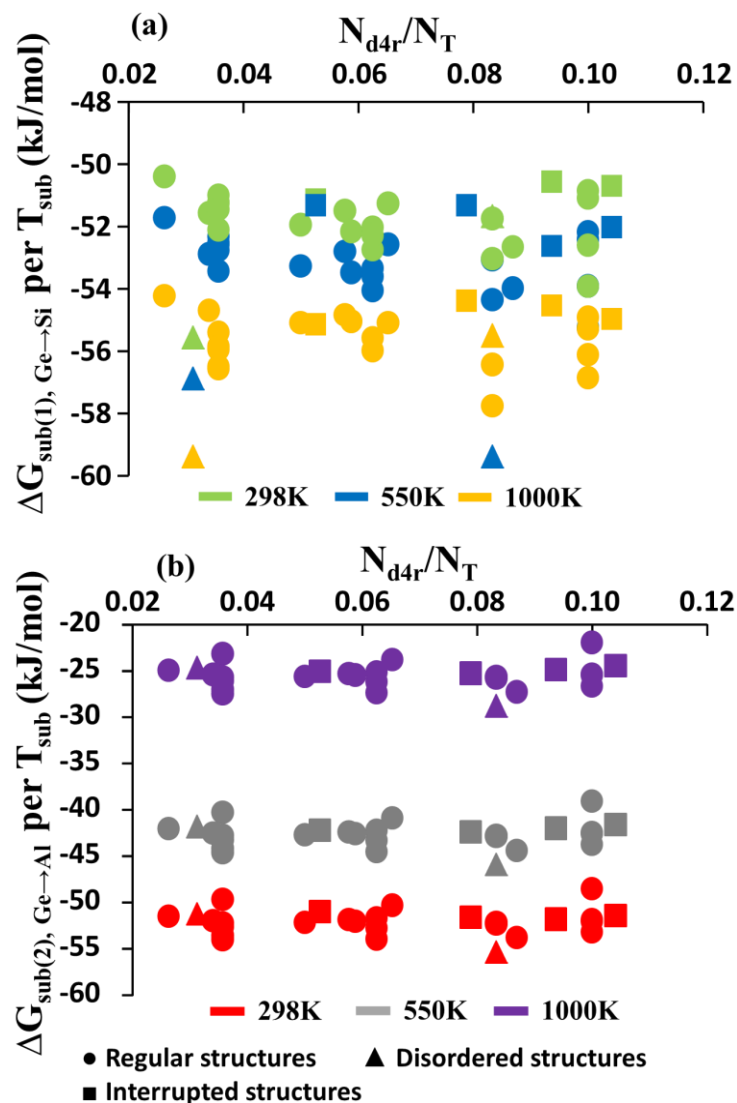


Figure 10: Gibbs free energies of substitution of Ge for Si ($\Delta G_{\text{sub}(1), \text{Ge} \rightarrow \text{Si}}$) departing from Ge occupying the full d4r (a) and Ge for Al ($\Delta G_{\text{sub}(2), \text{Ge} \rightarrow \text{Al}}$) departing from Ge occupying half of the d4r with alternation (b) at different temperatures, normalized to the number of substituted T sites against the number of d4r in the structures over the total T sites ($N_{\text{d4r}}/N_{\text{T}}$). Spheres, triangles and squares correspond to regular, partially disordered and interrupted structures, respectively.. Starting from parent silicogermanates with full-Ge-d4r, we calculated the energies of substitution of Ge for Si to obtain half-Ge-d4r silicogermanates (alternated /same s4r) or full silicate

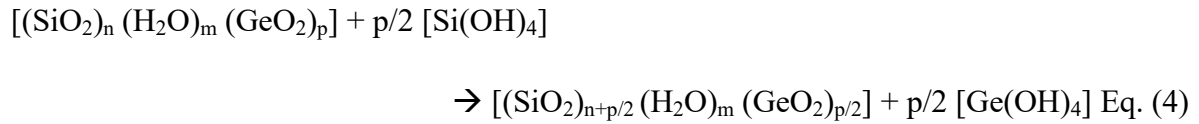
analogues ($\Delta E_{\text{sub}(1/2/3), \text{Ge} \rightarrow \text{Si}}$, represented with yellow arrows). Substitution of Ge by Al was evaluated starting either from full-Ge-d4r or both half-Ge-d4r ($\Delta E_{\text{sub}(1/2), \text{Ge} \rightarrow \text{Al}}$) respecting the Löwenstein rule. Finally, substitution of Si for Al was also evaluated ($\Delta E_{\text{sub}, \text{Si} \rightarrow \text{Al}}$).

The various substitution energies were calculated following the reactions given in equations 4-15 below.

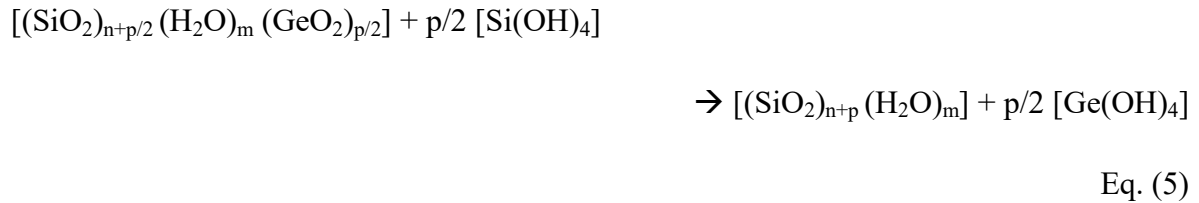
Using hydroxides:

❖ Ge→Si:

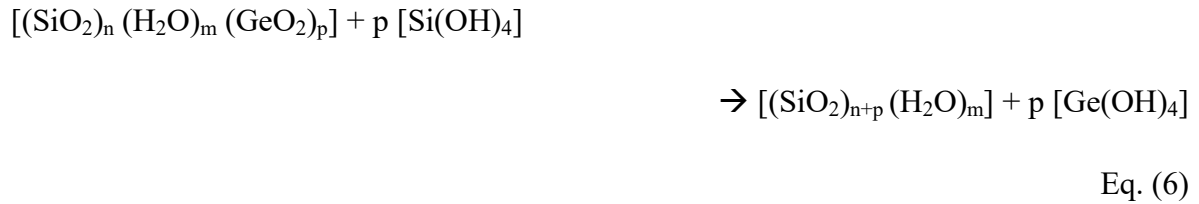
$\Delta E_{\text{sub}(1), \text{Ge} \rightarrow \text{Si}}$:



$\Delta E_{\text{sub}(2), \text{Ge} \rightarrow \text{Si}}$:

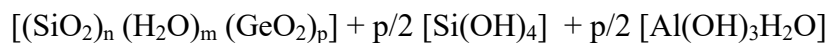


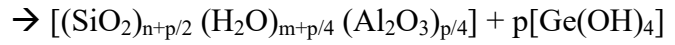
$\Delta E_{\text{sub}(3), \text{Ge} \rightarrow \text{Si}}$:



❖ Ge→Al:

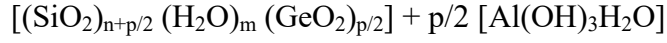
$\Delta E_{\text{sub}(1), \text{Ge} \rightarrow \text{Al}}$:





Eq. (7)

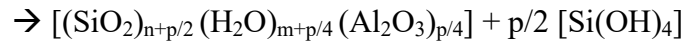
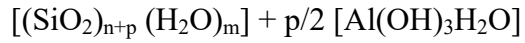
$\Delta E_{\text{sub (2), Ge} \rightarrow \text{Al}}$:



Eq. (8)

❖ $\text{Si} \rightarrow \text{Al}$:

$\Delta E_{\text{sub, Si} \rightarrow \text{Al}}$:

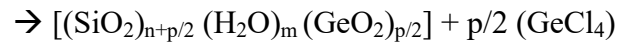


Eq. (9)

Using chlorides:

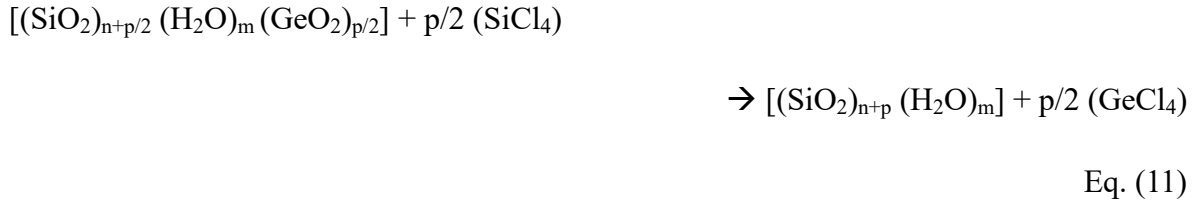
❖ $\text{Ge} \rightarrow \text{Si}$:

$\Delta E_{\text{sub (1), Ge} \rightarrow \text{Si}}$:



Eq. (10)

$\Delta E_{\text{sub (2), Ge} \rightarrow \text{Si}}$:

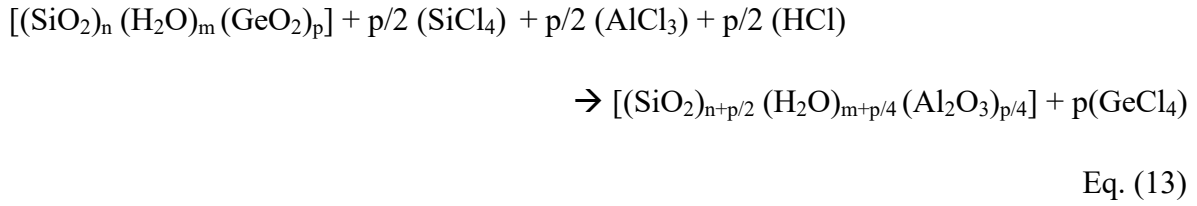


$\Delta E_{\text{sub (3), Ge} \rightarrow \text{Si}}$:

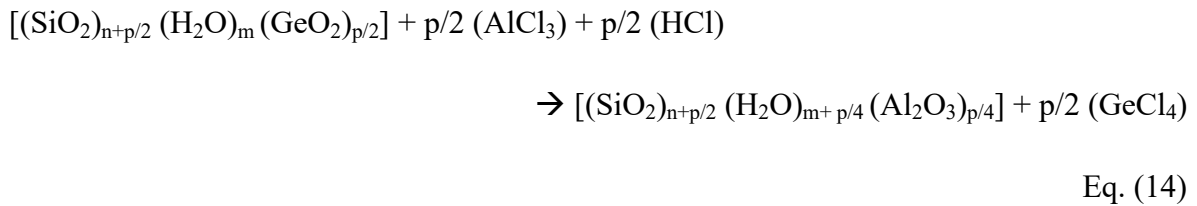


❖ $\text{Ge} \rightarrow \text{Al}$:

$\Delta E_{\text{sub (1), Ge} \rightarrow \text{Al}}$:

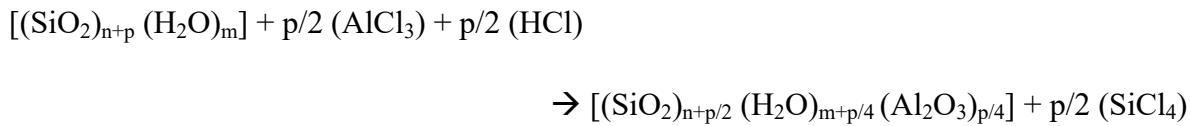


$\Delta E_{\text{sub (2), Ge} \rightarrow \text{Al}}$:



❖ $\text{Si} \rightarrow \text{Al}$:

$\Delta E_{\text{sub, Si} \rightarrow \text{Al}}$:



Eq.(15)

The values of $\Delta E_{\text{sub (3), Ge} \rightarrow \text{Si}}$ departing from a silicogermanate with Ge occupying the full d4r and $\Delta E_{\text{sub (2), Ge} \rightarrow \text{Al}}$ departing from Ge occupying half of the d4r with alternation are represented in Figure 7 (full removal of Ge). Both families of data follow a similar trend. All the energies of substitutions are negative, this means that thermodynamically the substitution of Ge for Si and Al should be possible using hydroxides or chlorides. In addition, almost no dependence between the substitution and the studied parameters nor the different zeolite structures exists. The results moreover indicate that substitution using chlorides is easier than using hydroxides.

The energetics of substitution were investigated on structures with Ge occupying entire d4r units, Ge occupying half of the d4r with alternation with Si or in s4r composing d4r, $\Delta E_{\text{sub (1, 2 and 3), Ge} \rightarrow \text{Si}}$ and $\Delta E_{\text{sub (1 and 2), Ge} \rightarrow \text{Al}}$. Changing the Ge organization was found not affecting the substitution energy since the energies of substitutions are almost overlapped (red and green, Figure 8).

The energies of substitution of Ge for Si or Al and even the energies of substitution of Si for Al per substituted atom indicate that these substitutions are almost independent of the population with the different atoms of the d4r of silicogermanates. In fact, the difference of these energies between all silicogermanates did not exceed 30 kJ/mol (Figure 8).

Moreover, it was found that the framework density does not differentiate zeolites with the same amount of d4rs. This is illustrated for zeolites with $N_{\text{d4r}}/N_{\text{T}}$ equal to 0.036 and 0.1 in Figure S3. In addition, in the latter zeolites, only small variations of the \widehat{OTO} angles in the d4r depending on chemical composition were noticed. The \widehat{OAlO} angles lie between 108

and 110° and the \widehat{OSiO} between 109 and 111° . This implies that the d4r units are uniform inside the different structures and are unconstrained by the density and the detailed framework structure of the zeolite. Sastre et al. predicted the feasibility of obtaining pure silica and germania zeolites by calculating an energetic penalty associated with \widehat{TOT} angles [98]. Based on that work, we measured the \widehat{TOT} (T= Si, Ge; Al) angles inside the d4r of the studied structures. The average \widehat{GeOGe} angle varied from 128 to 141° , that of \widehat{SiOGe} from 135 to 145° , the \widehat{SiOAl} ranges from 141 to 147° and \widehat{SiOSi} from 144 to 148° . As known, the ideal angles are 145 and 130° for \widehat{SiOSi} and \widehat{GeOGe} , respectively [108]. This indicates that Ge is crucial for the construction of the d4r having narrow angles. Once the framework is formed, its relaxation in the presence of other elements such as Al or Si is possible by the broadening of the \widehat{TOT} in the d4r. However, the stability of the structure is not directly related to the d4r angles, Figure 9. Furthermore, when the energy of substitution is reported against the difference of \widehat{TOT} angles between the initial and the substituted zeolite no correlation is noticed, Figure S4. These results indicate that the d4r itself is not responsible of the zeolite stability and its suitability for isomorphic substitution. The \widehat{TOT} effect can be related to the entire framework. Additionally, the average of the angles in the d4r does not correlate with the content of d4r of a structure (Figure 3). In other words, the intrinsic stability of the structures is not dependent of the characteristics of the d4r but of their number. In fact, the d4r units could create a tension on the surrounding angles. It is then possible that their number affects the strains exerted elsewhere in the network. These results are in agreement with the experimental enthalpies of high silica zeolites where the

enthalpies were not correlated to the average \widehat{SiOSi} angle but were critically dependent of the presence of an important amount of low \widehat{SiOSi} angles ($< 140^\circ$) [105].

Hence, an important conclusion from this theoretical study is that all reported silicogermanate zeolites are suited for isomorphic substitution of Ge with Si or Al atoms without significant distinction.

On the other hand, it is worth mentioning, that the average of $\Delta E_{\text{sub, Si} \rightarrow \text{Al}}$ per T substituted atom is -38 kJ/mol while that of $\Delta E_{\text{sub, Ge} \rightarrow \text{Al}}$ is -248 kJ/mol which highlights that substituting Ge for Al is energetically much more favorable than Si for Al (Figure 8). This suggests a preferential reactivity order during the isomorphic substitution post-treatment. For example, one could start by substituting partially Ge for Si to favor the conditions of respecting the Löwenstein rule in the next step of alumination. Then a treatment to substitute the remaining Ge for Al could follow. These treatments will then insure the stabilization of the material and the introduction of catalytic activity due to the presence of a newly introduced bridging OH groups.

The above energies are computed at 0 K. To obtain a more realistic description of experimental substitutions the Gibbs free energies (ΔG_{sub}) have also been calculated at temperatures varying from 298 K to 1000 K. The difference between these energies for normal and disordered structures does not exceed 20 kJ/mol so the temperature effect is small, Figure 10. Interestingly, substitution of Ge for Si becomes easier by increasing the temperature meanwhile working at lower temperature is preferable to substitute Ge for Al. Indeed, during the substitution of Ge for Al, adding an HCl molecule, Eq. (13-14), leads to

a loss of entropy. During the substitution of Ge for Si, the entropies of SiCl_4 and GeCl_4 are close hence the thermal effect is less pronounced.

4. Conclusions

According to our estimation of framework stability using DFT, silicate and aluminosilicate analogues of germanosilicate zeolites are thermodynamically more stable. This suggests that Ge plays a kinetic role during the crystallization of the zeolite. In addition, the intrinsic stability of germanosilicate zeolites is independent of the framework density. Substituting Ge for other elements such as Si and Al is feasible independently of the distribution of the d4r inside the different structures. This computational study suggests that large pore zeolites that currently can be synthesized with germanosilicate composition only can be converted to silicate and aluminosilicate variants by isomorphic substitution. These results open the door to future practical applications of a score of large pore zeolites with attractive pore structures. Energy estimations suggest the best procedure to be substitution of part of the Ge with silicon at high temperature in a first step, and substitution of the residual Ge with Al in a second step at lower temperature.

Appendix A. Supplementary Information

The supplementary information (S1) includes graphs and tables of cell parameters of the framework structures, electronic and Gibbs free energies and structural data for the BEC structure. (PDF)

The supplementary information (S2) includes CIF files of the studied structures in their silicate, silicogermanate (Ge occupying the full d4r, Ge occupying half of the d4r with alternation and Ge occupying half of the d4r in a same s4r) and aluminosilicate forms after geometric optimization. (.cif)

Acknowledgments

Nicolas Bats (formally IFP Energies Nouvelles, now Johnson Matthey) is acknowledged for fruitful discussions.

This work was performed using HPC resources from GENCI (Grant A0020806134) and the ENER440 cluster at IFP Energies nouvelles.

JAM acknowledges the Flemish government for long term structural funding (Methusalem).

References

- [1] J.V. Smith, *Chem. Rev.* 88 (1988) 149–182.
- [2] W. Vermeiren, J-P. Gilson, *Top. Catal.* 52 (2009) 1131–1161.
- [3] O. V. Shvets, N. Kasian, A. Zúkal, J. Pinkas, J. Čejka, *Chem. Mater.* 22 (2010) 3482–3495.
- [4] H. Xu, J.-G. Jiang, B. Yang, L. Zhang, M. He, P. Wu, *Angew. Chem.* 126 (2014) 1379–1383.
- [5] A. Corma, M. J. Diaz-Cabanas, J. L. Jorda, C. Martinez, M. Moliner, *Nature* 443 (2006) 842–845.
- [6] J. Jiang, Y. Xu, P. Cheng, Q. Sun, J. Yu, A. Corma, R. Xu, *Chem. Mater.* 23 (2011) 4709–4715.
- [7] P. A. Kots, A.V. Kurkin, V.L. Sushkevich, A.N. Fitch., V.V. Chernyshev, I. I. Ivanova, *CrystEngComm* 19 (2017) 5982–5988.
- [8] E. Verheyen, J. Lennart K. Van Havenbergh E. Breynaert, N. Kasian E. Gobechiya K. Houthoofd C. Martineau, M. Hinterstein, F. Taulelle V. Van Speybroeck, M. Waroquier S. Bals G Van Tendeloo C.E.A. Kirschhock., J.A. Martens, *Nat. Mater.* 11 (2012) 1059–1064.
- [9] Q. Li, A. Navrotsky, F. Rey, A. Corma, *Microporous Mesoporous Mater.* 59 (2003) 177–183.
- [10] F. Gao, M. Jaber, K. Bozhilov, A. Vicente, C. Fernandez, V. Valtchev, *J. Am. Chem. Soc.* 131 (2009) 16580–16586.
- [11] M. V. Shamzhy, P. Eliašová, D. Vitvarová, M. V. Opanasenko, D. S. Firth, R. E. Morris, *Chem. Eur. J.* 22 (2016) 17377–17386.
- [12] W.J. Roth, P. Nachtigall, R.E. Morris, J. Čejka, *Chem. Rev.* 114 (2014) 4807–4837.
- [13] M. Shamzhy, F. S. de O. Ramos, *Catal. Today* 243 (2015) 76–84.
- [14] V. Kasneryk, M. Opanasenko, M. Shamzhy, Z. Musilová, Y.S. Avadhut, M. Hartmann, J. Čejka, *J. Mater. Chem. A* 5 (2017) 22576–22587.
- [15] V. I. Kasneryk, M. V. Shamzhy, M. V. Opanasenko, J. Čejka, *J. Energy Chem.* 25 (2016) 318–326.
- [16] A. Rodríguez-Fernández, F. J. Llopis, C. Martínez, M. Moliner, A. Corma, *Microporous Mesoporous Mater.* 267 (2018) 35–42.
- [17] L. Burel, N. Kasian, A. Tuel, *Angew. Chem. Int. Ed.* 53 (2014) 1360–1363.
- [18] P. Chlubná-Eliášová, Y. Tian, A. B. Pinar, M. Kubů, J. Čejka, R. E. Morris, *Angew. Chem. Int. Ed.* 53 (2014) 7048–7052.
- [19] P. Eliašová, M. Opanasenko, P. S. Wheatley, M. Shamzhy, M. Mazur, P. Nachtigall, W. J. Roth, R. E. Morris, J. Čejka, *Chem. Soc. Rev.* 44 (2015) 7177–7206.
- [20] J.H. Kang, D. Xie, S.I. Zones, M.E. Davis, *Chem. Mater.* 32 (2020) 2014–2024.
- [21] P. St. Petkov, H. A. Aleksandrov, V. Valtchev, and G. N. Vayssilov, *Chem. Mater.* 24 (2012) 2509–2518.
- [22] Y. Wang, J. Song, H. Gies, *Solid State Sci.* 5 (2003) 1421–1433.
- [23] L.A. Villaescusa, P.A. Barrett, M.A. Camblor, *Chem. Mater.* 10 (1998) 3966–3973.
- [24] P. Caullet, J.L. Guth, J. Hazm, J.M. Lamblin, H. Gies, *Eur. J. Solid State Inorg. Chem.* 28 (1991) 345–361.
- [25] L.Q. Tang, M.S. Dadachov, X.D. Zou, pp. 739–745.

- [26] A. Cantín, A. Corma, M.J. Díaz-Cabañas, J.L. Jordá, M. Moliner, F. Rey, *Angew. Chem. Int. Ed.* 45 (2006) 8013–8015.
- [27] Z. Liu, T. Ohsuna, O. Terasaki, M.A. Camblor, M.J. Diaz-Cabañas, K. Hiraga, *J. Am. Chem. Soc.* 123 (2001) 5370–5371.
- [28] A. Corma, M. T. Navarro, F. Rey, J. Rius, S. Valencia, *Angew. Chem. Int. Ed.* 40 (2001) 2277–2280.
- [29] J.-Q. Song, B. Marler, H. Gies, *Compt. Rend. Chimie* 8 (2005) 341–352.
- [30] S. Leiva, M.J. Sabater, S. Valencia, G. Sastre, V. Fornés, F. Rey, A. Corma, *Compt. Rend. Chimie* 8 (2005) 369–378.
- [31] *Angew. Chem. Int. Ed.* 38 (1999) 1997–2000.
- [32] T. Blasco, A. Corma, M.J. Díaz-Cabañas, F. Rey, J. A. Vidal-Moya, C. M. Zicovich-Wilson, *J. Phys. Chem. B* 106 (2002) 2634–2642.
- [33] Y. Bouizi, J.-L. Paillaud, L. Simon, V. Valtchev, *Chem. Mater.* 19 (2007) 652–654.
- [34] A. CORMA, F. Rey, J. Rius, M.J. Sabater, S. Valencia, *Nature* 431 (2004) 287–290.
- [35] L. Tang, X. Ren, A.K. Inge, T. Willhammar, D. Grüner, J. Yu, X. Zou.
- [36] G.T. Kokotailo, S.L. Lawton, D.H. Olson, W.M. Meier, *Nature* 272 (1978) 437–438.
- [37] E.M. Flanigen, J.M. Bennett, R.W. Grose, J.P. Cohen, R.L. Patton, R.M. Kirchner, J.V. Smith, *Nature* 271 (1978) 512–516.
- [38] Y. Chen, S. Huang, X. Wang, L. Zhang, N. Wu, F. Liao, Y. Wang, *Cryst. Growth Des.* 17 (2017) 5465–5473.
- [39] E. Galli, G. Gottardi, *Miner. Petrogr. Acta* 12 (1966) 1–10.
- [40] T. Conradsson, M.S. Dadachov, X.D. Zou, *Microporous Mesoporous Mater.* 41 (2000) 183–191.
- [41] A. Corma, M. T. Navarro, F. Rey, S. Valencia, *Chem. Commun.* 0 (2001) 1486–1487.
- [42] L. Shi, Y. Yuan, N. Zhang, S. Lin, T. Yu, J. Wang, *J. Porous. Mater.* 23 (2016) 647–654.
- [43] K. Jiao, Z. Zhang, X. Xu, Z. Lv, J. Song, C. Lin, J. Sun, M. He, H. Gies, *Dalton Trans.* 46 (2017) 2270–2280.
- [44] M. Hernández-Rodríguez, J. L. Jordá, F. Rey, A. Corma, *J. Am. Chem. Soc.* 134 (2012) 13232–13235.
- [45] J. Jiang, J. L. Jorda, M. J. Diaz-Caban, J. Yu, A. Corma, *Angew. Chem. Int. Ed.* 49 (2010) 4986–4988.
- [46] K. Qian, Y. Wang, Z. Liang, J. Li, *RSC Adv.* 5 (2015) 63209–63214.
- [47] R. Bai, Q. Sun, N. Wang, Y. Zou, G. Guo, S. Iborra, A. Corma, J. Yu, *Chem. Mater.* 28 (2016) 6455–6458.
- [48] M. Moliner, T. Willhammar, W. Wan, J. González, F. Rey, J. L. Jorda, X. Zou, A. Corma, *J. Am. Chem. Soc.* 134 (2012) 6473–6478.
- [49] A. Corma, M.J. Diaz-Caban, J.L. Jorda, F. Rey, G. Sastre, K.G. Strohmaier, *J. Am. Chem. Soc.* 130 (2008) 16482–16483.
- [50] A. Corma, M.J. Diaz-Caban, J.L. Jorda, F. Rey, K. Boulahya, J.M. Gonzalez-Calbet, *J. Phys. Chem. C* 113 (2009) 9305–9308.
- [51] A. Corma, M.J. Díaz-Cabañas, J.L. Jordá, C. Martínez, M. Moliner, *Nature* 443 (2006) 842–845.
- [52] A. Corma, M. Moliner, M. J. Diaz-Caban, J. M. Serra Alfaro, R. Castañeda European Patent 1847510A1(2006).

- [53] M. Bjørgen, A.H. Grave, Saepurahman, A. Volynkin, K. Mathisen, K.P. Lillerud, U. Olsbye, S. Svelle, *Microporous Mesoporous Mater.* 151 (2012) 424–433.
- [54] Q. Kun, S. Xiao-Wei, X. Da, L. Ji-Yang, *Chem. J. Chinese U.* 33 (2012) 2141–2145.
- [55] L. Liu, Z.-B. Yu, H. Chen, Y. Deng, B.-L. Lee, J. Sun, *Cryst. Growth Des.* 13 (2013) 4168–4171.
- [56] L. Wu, J. Hughes, M. Moliner, A. Navrotsky, A. Corma, *Microporous Mesoporous Mater.* 187 (2014) 77–81.
- [57] Z. Zhang, Y. Guo, X. Liu, *J. Phys. Chem. C* 121 (2017) 11568–11575.
- [58] R. Castañeda, A. Corma, V. Fornés, F. Rey, J. Rius, *J. Am. Chem. Soc.* 125 (2003) 7820–7821.
- [59] A. Cantín, A. Corma, M. J. Díaz-Cabanas, J. L. Jordá, M. Moliner, *J. Am. Chem. Soc.* 128 (2006) 4216–4217.
- [60] W. H. Fu, Z. Yuan, Z. Wang, Y. Wang, W. Yang, M. Y. He, *Dalton Trans.* 46 (2017) 6692–6699.
- [61] D.L. Dorset, K.G. Strohmaier, C.E. Kliewer, A. Corma, M.J. Díaz-Cabañas, F. Rey, C.J. Gilmore, *Chem. Mater.* 20 (2008) 5325–5331.
- [62] A. Corma, F. Rey, S. Valencia, J.L. Jordá, J. Rius, *Nat. Mater.* 2 (2003) 493–497.
- [63] G. Sastre, A. Pulido, R. Castañeda, A. Corma, *J. Phys. Chem. B* 108 (2004) 8830–8835.
- [64] X. Liu, U. Ravon, F. Bosselet, G. Bergeret, A. Tuel, *Chem. Mater.* 24 (2012) 3016–3022.
- [65] R. Yuan, N. Claes, E. Verheyen, A. Tuel, S. Bals, E. Breynaert, J.A. Martens, C.E.A. Kirschhock, *New J. Chem.* 40 (2016) 4319–4324.
- [66] W. Hua, H. Chen, Z.-B. Yu, X. Zou, J. Lin, J. Sun, *Angew. Chem. Int. Ed.* 53 (2014) 5868–5871.
- [67] L. Tang, L. Shi, C. Bonneau, J. Sun, H. Yue, A. Ojuva, B.-L. Lee, M. Kritikos, R.G. Bell, Z. Bacsik, J. Mink, X. Zou, *Nat. Mater.* 7 (2008) 381–385.
- [68] Y. Luo, S. Smeets, F. Peng, A.S. Etman, Z. Wang, J. Sun, W. Yang, *Chem. Eur. J.* 23 (2017) 16829–16834.
- [69] L. Bieseki, R. Simancas, J.L. Jordá, P.J. Bereciartua, Á. Cantín, J. Simancas, S.B. Pergher, S. Valencia, F. Rey, A. Corma, *Chem. Commun.* 54 (2018) 2122–2125.
- [70] N. Zhang, L. Shi, T. Yu, T. Li, W. Hua, C. Lin, *J. Solid State Chem.* 225 (2015) 271–277.
- [71] D.J. Earl, A.W. Burton, T. Rea, K. Ong, M.W. Deem, S.-J. Hwang, S.I. Zones, *J. Phys. Chem. C* 112 (2008) 9099–9105.
- [72] L.B. McCusker, C. Baerlocher, A.W. Burton, S.I. Zones, *Solid State Sci.* 13 (2011) 800–805.
- [73] Y. Lorgouilloux, M. Dodin, J.-L. Paillaud, P. Caullet, L. Michelin, L. Josien, O. Ersen, N. Bats, *J. Solid State Chem.* 182 (2009) 622–629.
- [74] Y. Lorgouilloux, M. Dodin, E. Mugnaioli, C. Marichal, P. Caullet, N. Bats, U. Kolb, J.-L. Paillaud, *RSC Adv.* 4 (2014) 19440–19449.
- [75] Y. Mathieu, J.-L. Paillaud, P. Caullet, N. Bats, *Microporous Mesoporous Mater.* 75 (2004) 13–22.
- [76] J.-L. Paillaud, B. Harbuzaru, J. Patarin, N. Bats, *Science* 304 (2004) 990–992.
- [77] O.V. Shvets, A. Zukal, N. Kasian, N. Zilková, J. Cejka, *Chem. Eur. J.* 14 (2008) 10134–10140.
- [78] A. Corma, M.J. Diaz-Cabanas, F. Rey, S. Nicolopoulos, K. Boulahya, *Chem. Commun.* (2004) 1356–1357.

- [79] M. Dodin, J.-L. Paillaud, Y. Lorgouilloux, P. Caullet, E. Elkaïm, N. Bats, *J. Am. Chem. Soc.* 132 (2010) 10221–10223.
- [80] J. Sun, C. Bonneau, A. Cantín, A. Corma, M.J. Díaz-Cabañas, M. Moliner, D. Zhang, M. Li, X. Zou, *Nature* 458 (2009) 1154–1157.
- [81] K. Qian, J. Li, J. Jiang, Z. Liang, J. Yu, R. Xu, *Microporous Mesoporous Mater.* 164 (2012) 88–92.
- [82] F.-J. Chen, Z.-H. Gao, L.-L. Liang, J. Zhang, H.-B. Du, *CrystEngComm* 18 (2016) 2735–2741.
- [83] Y. Yun, M. Hernandez, W. Wan, X. Zou, J. L. Jorda, A. Cantin, F. Rey, A. Corma, *Chem. Commun.* 51 (2015) 7602–7605.
- [84] J. Jiang, Y. Yun, X. Zou, J. L. Jorda, A. Corma, *Chem. Sci.* 6 (2015) 480–485.
- [85] A. Corma, M. J. Diaz-Cabanias, J. Jiand, D. L. Dorset, S. L. Soled, K. G. Strohmaier, *PNAS* 107 (2010) 13997–14002.
- [86] Z.-H. Gao, F.-J. Chen, L. Xu, L. Sun, Y. Xu, H.-B. Du, *Chem. Eur. J.* 22 (2016) 14367–14372.
- [87] B.W. Boal, M.W. Deem, D. Xie, J.H. Kang, M.E. Davis, S.I. Zones, *Chem. Mater.* 28 (2016) 2158–2164.
- [88] J.H. Kang, D. Xie, S.I. Zones, S. Smeets, L.B. McCusker, M.E. Davis, *Chem. Mater.* 28 (2016) 6250–6259.
- [89] D.S. Firth, S.A. Morris, P.S. Wheatley, S.E. Russell, A.M.Z. Slawin, D.M. Dawson, A. Mayoral, M. Opanasenko, M. Položij, J. Čejka, P. Nachtigall, R.E. Morris, *Chem. Mater.* 29 (2017) 5605–5611.
- [90] G. Kresse, J. Hafner, *Phys. Rev. B* (1994) 14251–14269.
- [91] G. Kresse, J. Furthmüller, *Comput. Mater. Sci.* 6 (1996) 15–50.
- [92] J. P. Perdew, K. Burke, M. Ernzerhof, *Phys. Rev. Lett.* (1996) 3865–3868.
- [93] S.N. Steinmann, C. Corminboeuf, *J. Chem. Theory Comput.* 7 (2011) 3567–3577.
- [94] G. Kresse, D. Joubert, *Phys. Rev. B* (1999) 1758–1775.
- [95] <http://www.iza-online.org/>.
- [96] K. Larmier, C. Chizallet, N. Cadran, S. Maury, J. Abboud, A.-F. Lamic-Humblot, E. Marceau, H. Lauron-Pernot, *ACS Catal.* 5 (2015) 4423–4437.
- [97] C.J. Dawson, R. Sanchez-Smith, P. Rez, M. O’Keeffe, M.M.J. Treacy, *Chem. Mater.* 26 (2014) 1523–1527.
- [98] G. Sastre, A. Corma, *J. Phys. Chem. C* 114 (2010) 1667–1673.
- [99] W. Loewenstein, *Am. Min.* 39 (1954) 92–96.
- [100] Q. Li, A. Navrotsky, F. Rey, A. Corma, *Microporous Mesoporous Mater.* 74 (2004) 87–92.
- [101] J. Haines, O. Cambon, E. Philippot, L. Chapon, S. Hull, *J. Solid State Chem.* 166 (2002) 434–441.
- [102] Y.G. Bushuev, G. Sastre, *J. Phys. Chem. C* 114 (2010) 19157–19168.
- [103] R.A. van Santen, G.J. Kramer, *Chem. Rev.* 95 (1995) 637–660.
- [104] G. J. Kramer, A. J. M. de Man, R. A. van Santen, *J. Am. Chem. Soc.* 113 (1991) 6435–6441.
- [105] I. Petrovic, A. Navrotsky, M. E. Davis, S. I. Zones, *Chem. Mater.* 5 (1993) 1805–1813.

- [106] G. Sastre, J. A. Vidal-Moya, T. Blasco, J. Rius, J. L. Jordá, M. T. Navarro, F. Rey, A. Corma, *Angew. Chem. Int. Ed.* 41 (2002) 4722–4726.
- [107] G. Sastre, A. Pulido, A. Corma, *Microporous Mesoporous Mater.* 82 (2005) 159–163.
- [108] M. O. Keeffe, O.M. Yaghi, *Chem. Eur. J.* 5 (1999) 2796–2801.
- [109] Y. Luo, S. Smeets, Z. Wang, J. Sun, W. Yang, *Chemistry (Weinheim an der Bergstrasse, Germany)* 25 (2019) 2184–2188.
- [110] M.O. Cichocka, Y. Lorgouilloux, S. Smeets, J. Su, W. Wan, P. Caullet, N. Bats, L.B. McCusker, J.-L. Paillaud, X. Zou, *Cryst. Growth Des.* 18 (2018) 2441–2451.

Tables:

Table 1: List of structure types investigated in the present work. The names correspond to zeolites in their silicogermanate forms.

IZA Structural code	Name	K-points mesh
Regular		
ASV [25]	SU-10	3x3x1
BEC [28,41–43]	ITQ-17	Γ point
IRN [44]	ITQ-49	Γ point
IRR [6,45–47]	ITQ-44	Γ point
ITG [48]	ITQ-38	Γ point
ITR [49,50]	ITQ-34	Γ point
ITT [51–57]	ITQ-33	Γ point
IWR [58–60]	ITQ-24	Γ point
IWS [61]	ITQ-26	Γ point
IWW [62–65]	ITQ-22	Γ point
POS [66]	PKU-16	Γ point
SOF [67]	SU-15	1x1x2
SOR [68,69]	SCM-14;ITQ-62	1x1x11
STW [67,70]	SU-32 ;Ge-STW	Γ point
SOV [109]	SCM-15	Γ point
SVV [71,72]	SSZ-77	Γ point

UOS [73]	IM-16	1x4x4
UOV [74]	IM-17	Γ point
UOZ [75]	IM-10	4x4x1
UTL [3,76–78]	IM-12 ;ITQ-15	Γ point
UWY [79]	IM-20	Γ point
Interrupted		
-IFT [83]	ITQ-53	Γ point
-IFU [84]	ITQ-54	Γ point
-IRY [85]	ITQ-40	Γ point
-ITV [6,80–82]	ITQ-37	Γ point
Partially Disordered		
*CTH [86–89]	CIT-13 ;NUD-2; SAZ-1	Γ point
*UOE [110]	IM-18	3x3x1

(-) for interrupted, (*) for partially disordered structures.

Figure Captions

Figure 1: Ge and Si siting in d4r units: (a) Ge occupying all d4r, (b) Ge occupying half of the d4r with alternation with Si and (c) Ge occupying half of the d4r in a same s4r. [The d4r part of the structures only are shown, the other parts of the structure \(with T sites occupied by Si only\) are omitted for the sake of clarity and for generalization purposes.](#)

Figure 2: Al and Si siting in aluminosilicate d4r units.

Figure 3: Energies of formation per T site ($\Delta E_{\text{form}}/N_{\text{T}}$) of silicates (yellow), silicogermanates with Ge occupying the full d4r (green) and aluminosilicates (purple) of (a) regular (circles), partially disordered (triangles) and (b) interrupted (squares) zeolite structures. $N_{\text{d4r}}/N_{\text{T}}$ correspond to the number of d4r of the structure over the total number of T sites.

Figure 4: Variation of the framework density against the ratio of the number of d4r units in the structure over the total T sites ($N_{\text{d4r}}/N_{\text{T}}$). The studied framework types are represented in Table 1.

Figure 5: Positioning of d4r in UTL, UOZ and ITT framework structures. For UTL and ITT, only single 4-rings of the d4r units occupied by Ge atoms are shown for clarity.

Figure 6: Substitution scheme of Ge for Si and Al using chlorides. [The d4r part of the structures only are shown, the other parts of the structure \(with T sites occupied by Si only\) are omitted for the sake of clarity and for generalization purposes.](#)

Figure 7: Energies of full substitution of Ge for Si ($\Delta E_{\text{sub (3), Ge} \rightarrow \text{Si}}$) departing from Ge occupying the full d4r (yellow) and of Ge for Al ($\Delta E_{\text{sub (2), Ge} \rightarrow \text{Al}}$) departing from Ge occupying half of the d4r with alternation (purple), normalized to the number of substituted T sites, using (a) hydroxides and (b) chlorides against the number of d4r in the structures over the total T sites ($N_{\text{d4r}}/N_{\text{T}}$). Spheres, triangles and squares correspond to regular, partially disordered and interrupted zeolite structures, respectively.

Figure 8: Energies of partial substitution of Ge for Si $\Delta E_{\text{sub}(1), \text{Ge} \rightarrow \text{Si}}$ departing from full occupation of d4r with Ge and full substitution $\Delta E_{\text{sub}(2,3), \text{Ge} \rightarrow \text{Si}}$ departing from Ge occupying half/same s4r and fully in the d4r respectively(a). Energies of partial substitution of Ge for Al $\Delta E_{\text{sub}(1), \text{Ge} \rightarrow \text{Al}}$ departing from Ge occupying the full d4r and full substitution $\Delta E_{\text{sub}(2), \text{Ge} \rightarrow \text{Al}}$ departing from Ge occupying half of the d4r with alternation or in the same s4r (b). Energies of full substitution of Si for Al $\Delta E_{\text{sub}, \text{Si} \rightarrow \text{Al}}$ departing from Al occupying half of the d4r (c). All the energies are normalized to the number of substituted T sites against the number of d4r in the structures over the total T sites ($N_{\text{d4r}}/N_{\text{T}}$). Spheres, triangles and squares correspond to regular, partially disordered and interrupted structures respectively.

Figure 9: Energies of formation per T sites ($\Delta E_{\text{form}}/ \text{T sites}$) of silicates (yellow), silicogermanates with Ge occupying the full d4r (dark green)/ Ge occupying half of the d4r with alternation (light green) and aluminosilicates (purple) of all studied structures. **TOT** correspond to angles in the d4r respectively **SiOSi**, **GeOGe**, **SiOGe** and **SiOAl**.

Figure 10: Gibbs free energies of substitution of Ge for Si ($\Delta G_{\text{sub}(1), \text{Ge} \rightarrow \text{Si}}$) departing from Ge occupying the full d4r (a) and Ge for Al ($\Delta G_{\text{sub}(2), \text{Ge} \rightarrow \text{Al}}$) departing from Ge occupying half of the d4r with alternation (b) at different temperatures, normalized to the number of substituted T sites against the number of d4r in the structures over the total T sites ($N_{\text{d4r}}/N_{\text{T}}$). Spheres, triangles and squares correspond to regular, partially disordered and interrupted structures, respectively.

Figures:

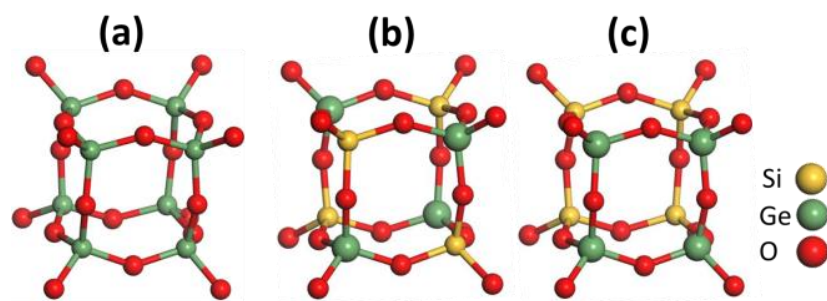


Figure 1: Ge and Si siting in d4r units: (a) Ge occupying all d4r, (b) Ge occupying half of the d4r with alternation with Si and (c) Ge occupying half of the d4r in a same s4r. The d4r part of the structures only are shown, the other parts of the structure (with T sites occupied by Si only) are omitted for the sake of clarity and for generalization purposes.

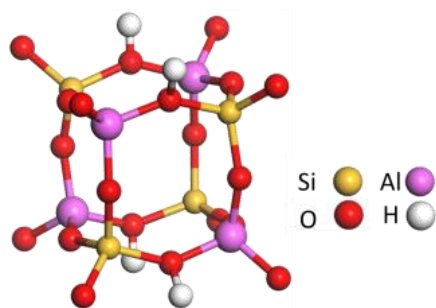


Figure 2: Al and Si siting in aluminosilicate d4r units.

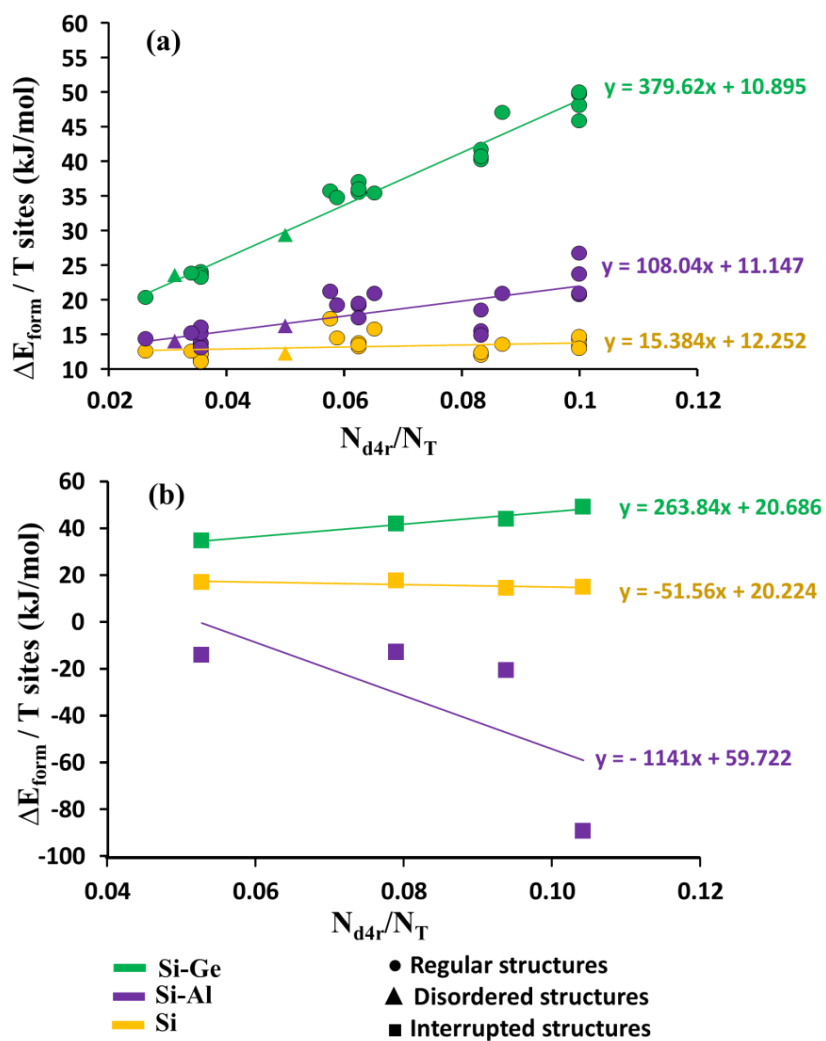


Figure 3: Energies of formation per T site ($\Delta E_{\text{form}} / \text{T sites}$) of silicates (yellow), silicogermanates with Ge occupying the full d4r (green) and aluminosilicates (purple) of (a) regular (circles), partially disordered (triangles) and (b) interrupted (squares) zeolite structures. $N_{\text{d4r}} / N_{\text{T}}$ correspond to the number of d4r of the structure over the total number of T sites.

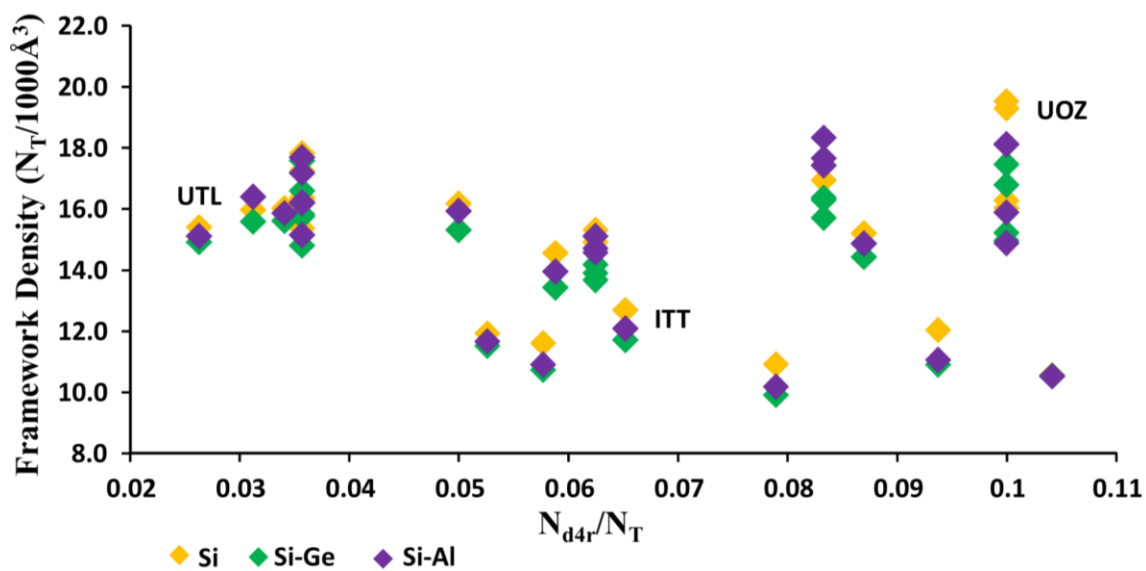


Figure 4: Variation of the framework density against the ratio of the number of d4r units in the structure over the total T sites (N_{d4r}/N_T). The studied framework types are represented in Table 1.

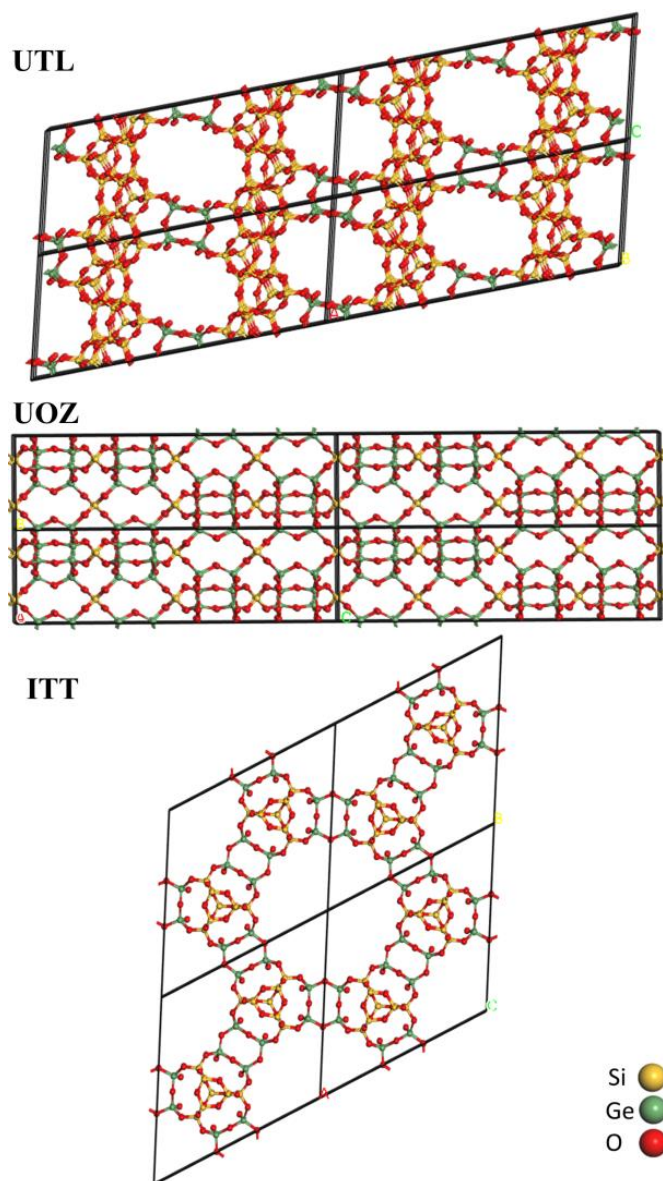


Figure 5: Positioning of d4r in UTL, UOZ and ITT framework structures. For UTL and ITT, only single 4-rings of the d4r units occupied by Ge atoms are shown for clarity.

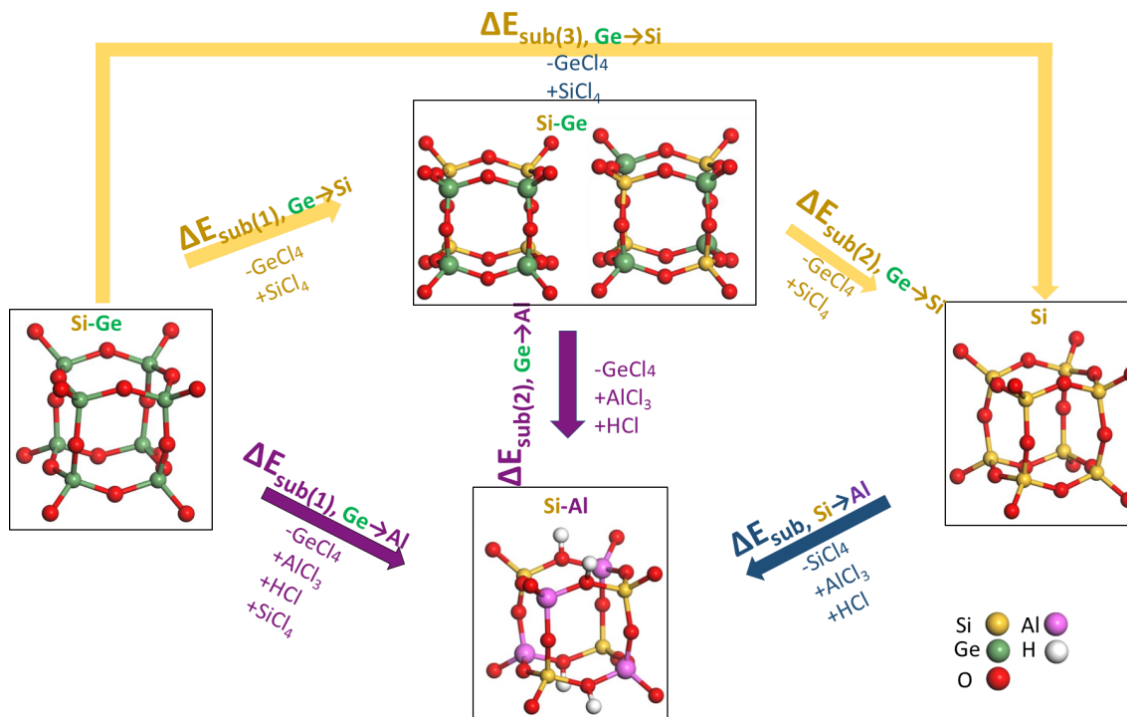


Figure 6: Substitution scheme of Ge for Si and Al using chlorides. The d4r part of the structures only are shown, the other parts of the structure (with T sites occupied by Si only) are omitted for the sake of clarity and for generalization purposes.

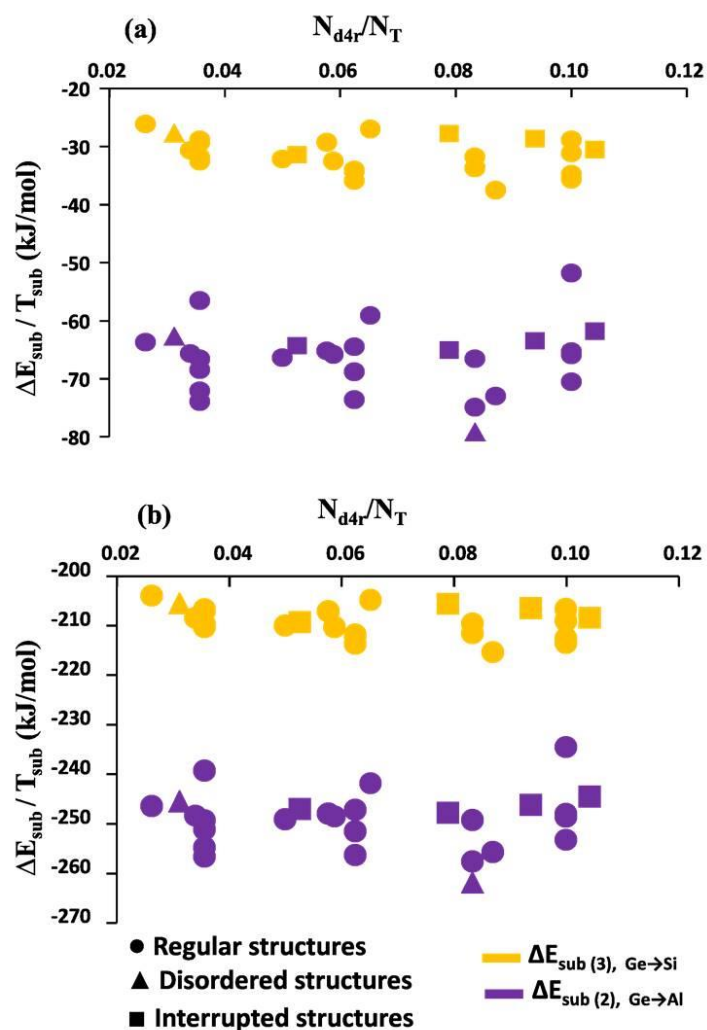


Figure 7: Energies of full substitution of Ge for Si ($\Delta E_{\text{sub}}(3), \text{Ge} \rightarrow \text{Si}$) departing from Ge occupying the full d4r (yellow) and of Ge for Al ($\Delta E_{\text{sub}}(2), \text{Ge} \rightarrow \text{Al}$) departing from Ge occupying half of the d4r with alternation (purple), normalized to the number of substituted T sites, using (a) hydroxides and (b) chlorides against the number of d4r in the structures over the total T sites (N_{d4r}/N_T). Spheres, triangles and squares correspond to regular, partially disordered and interrupted zeolite structures, respectively.

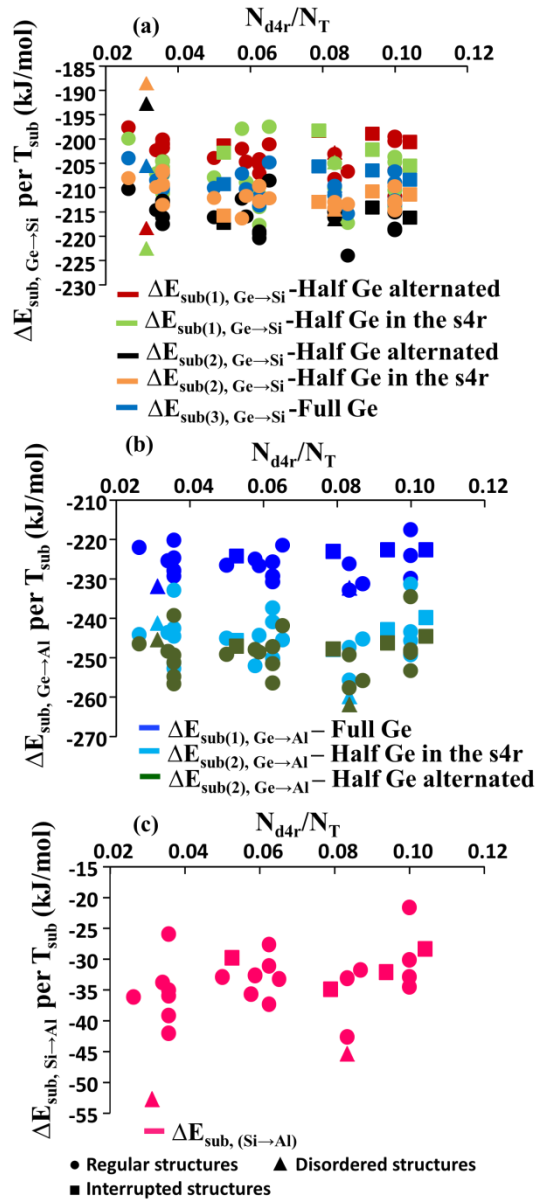


Figure 8: Energies of partial substitution of Ge for Si $\Delta E_{\text{sub}(1), \text{Ge} \rightarrow \text{Si}}$ departing from full occupation of d4r with Ge and full substitution $\Delta E_{\text{sub}(2,3), \text{Ge} \rightarrow \text{Si}}$ departing from Ge occupying half/same s4r and fully in the d4r respectively(a). Energies of partial substitution of Ge for Al $\Delta E_{\text{sub}(1), \text{Ge} \rightarrow \text{Al}}$ departing from Ge occupying the full d4r and full substitution $\Delta E_{\text{sub}(2), \text{Ge} \rightarrow \text{Al}}$ departing from Ge occupying half of the d4r with alternation or in the same s4r (b). Energies of full substitution of Si for Al $\Delta E_{\text{sub, Si} \rightarrow \text{Al}}$ departing from Al occupying half of the d4r (c). All the energies are normalized to the number of substituted T sites against the number of d4r in the structures over the total T sites (N_{d4r}/N_T). Spheres, triangles and squares correspond to regular, partially disordered and interrupted structures respectively.

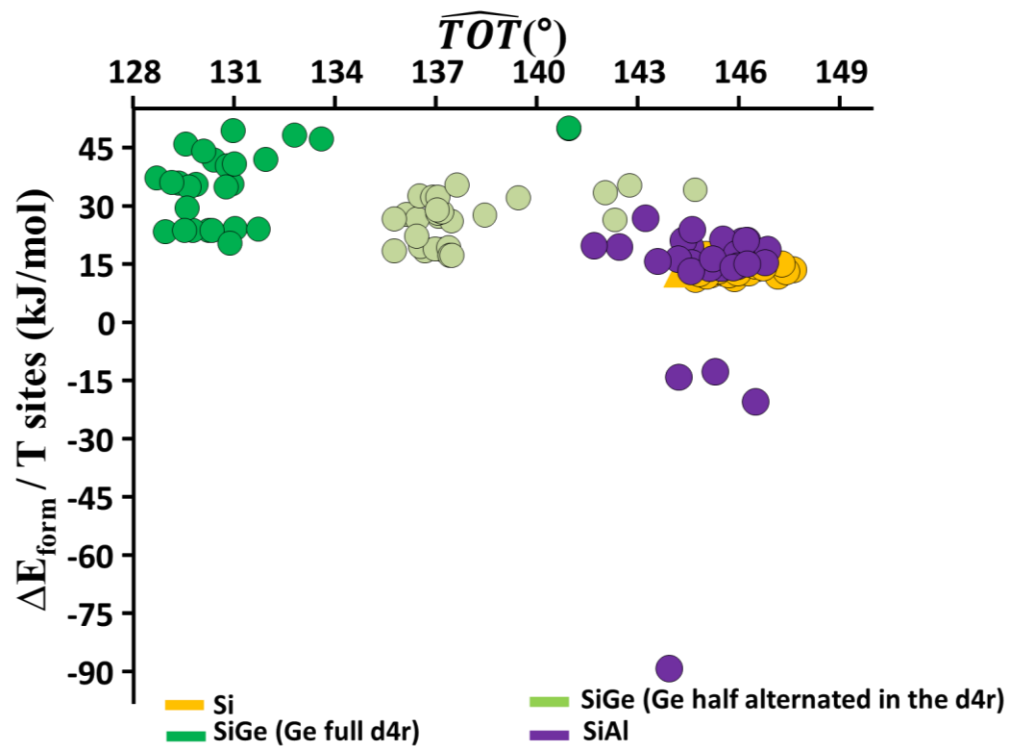


Figure 9: Energies of formation per T sites ($\Delta E_{\text{form}} / \text{T sites}$) of silicates (yellow), silicogermanates with Ge occupying the full d4r (dark green)/ Ge occupying half of the d4r with alternation (light green) and aluminosilicates (purple) of all studied structures. \widehat{TOT} correspond to angles in the d4r respectively \widehat{SiOSi} , \widehat{GeOGe} , \widehat{SiOGe} and \widehat{SiOAl} .

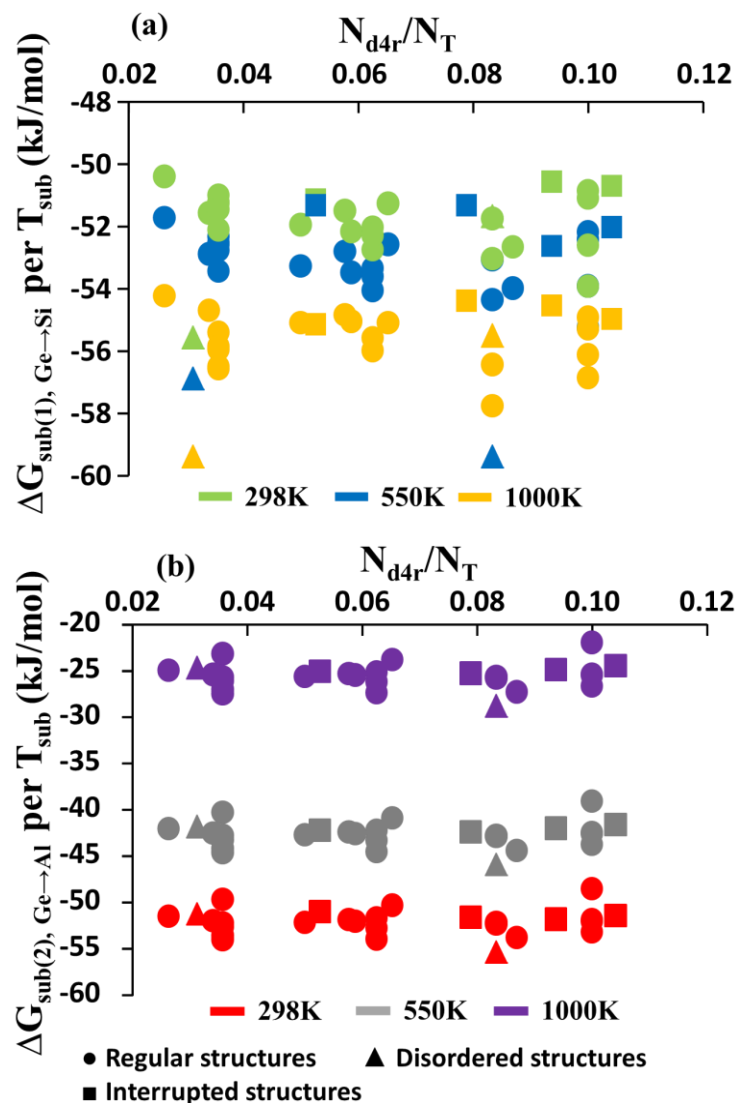


Figure 10: Gibbs free energies of substitution of Ge for Si ($\Delta G_{\text{sub}(1), \text{Ge} \rightarrow \text{Si}}$) departing from Ge occupying the full d4r (a) and Ge for Al ($\Delta G_{\text{sub}(2), \text{Ge} \rightarrow \text{Al}}$) departing from Ge occupying half of the d4r with alternation (b) at different temperatures, normalized to the number of substituted T sites against the number of d4r in the structures over the total T sites ($N_{\text{d4r}}/N_{\text{T}}$). Spheres, triangles and squares correspond to regular, partially disordered and interrupted structures, respectively.